New methods for image guidance and visualization for cardiac procedures

Michael A. Guttman, MS, Elliot R. McVeigh, PhD
Laboratory of Cardiac Energetics, NHLBI, National Institutes of Health
Department of Health and Human Services, Bethesda, MD

ABSTRACT

Interventional cardiac MRI has been undergoing rapid development because of the availability of MRI compatible interventional catheters, and the increased performance of the MRI systems. Intravascular techniques do not require an open access scanner, and hence higher imaging performance during procedures can be achieved. Now, with the availability of a short, relatively open cylindrical bore scanner high imaging performance is also available to guide direct surgical procedures.

1. INTRODUCTION

MRI gives the physician continuous imaging of soft tissues during an interventional procedure, which enables accurate targeting and precise titration of the delivery of therapy. Because the groin is accessible for femoral access, intravascular techniques do not require an open access scanner (such as a "double doughnut" or "clamshell" design [1,2]), and hence higher imaging performance during procedures can be achieved. Now, with the availability of a short, relatively open cylindrical bore scanner (Espree, Siemens), high imaging performance is also available to guide minimally invasive surgical procedures.

Over the past decade a number of MRI guided catheter based applications have been developed. Real-time display of the catheter position on 3D-MRI is useful for navigating a catheter towards a target tissue, such as the IVC, the fossa ovalis, and the left atrium for RF ablation. Real-time MRI also offers the physician the ability to monitor the size of the RF lesions through direct imaging of the signal enhancement after the tissue is heated.[3-5] Other applications include delivery and immediate visualization of intramyocardial injections of stem cells mixed with a contrast agent [6-8], renal artery stenting [9], and others [10,11]. Small independent receiver coils can be mounted on devices and used for device tracking [12,13] or creating high resolution images of tissue just next to the small coils [14,15]. The coil locations may be visualized by colorizing images reconstructed from the mounted device coil signal and blending them with grayscale images produced from surface coil signals [16-19]. The color-highlighted images indicate the positions of invasive devices with anatomical context. The acquisition of multiple slices can be interleaved and their relative orientation displayed in real time in a 3D viewer. [18,19].

Many of the techniques used for intravascular interventions can be applied directly to the guidance of minimally invasive surgical procedures. For some surgical procedures such as heart valve replacement and repair, percutaneous intravascular approaches [20,21] are under active investigation as well as minimally invasive surgical approaches. These approaches present different balances between risk and benefit. The open-chest surgical approach is associated with higher morbidity, but direct access allows superior visualization of anatomy and manipulation of devices for a more durable therapy. The percutaneous approaches reduce trauma, but therapeutic devices must be designed for catheter delivery through blood vessels, a constraint which may compromise the performance and durability of the device and therapy. In addition, some patients with stenotic cardiovascular disease may not be candidates for the percutaneous approach. With a minimally invasive surgical approach, it may be possible to achieve the best of both surgical and percutaneous approaches: reduce trauma while providing durable therapy. Recently, a novel surgical procedure in which real-time magnetic resonance imaging was used to interactively guide the placement of a prosthetic aortic valve in the beating heart via direct apical access was demonstrated.   Using interactive real-time MRI, the surgeon positioned the prosthetic valve in the correct location at the aortic annulus within 90 seconds. Ventricular function, blood flow through the valve, and myocardial perfusion were immediately evaluated with MRI.

2. CARDIAC INTERVENTIONAL MR IMAGING SYSTEM

2.1 New Magnet Configuration

A new 1.5T magnet design has recently become available; it is a closed bore designs with shorter depth and wider opening (Espree, Siemens Medical Solutions). It has a 120cm long bore which is 70cm wide; this provides greater accessibility with only a ~20% loss in imaging speed. Imaging field-of-view (FOV) is reduced to 30cm, but has been demonstrated to be adequate for many cardiac interventions. This magnet bore is short enough for a surgeon to reach the center of the magnet, and wide enough to allow placement and manipulation of instruments over the patient's body. With the heart positioned at the center of the magnet, the short bore also allows better access to the head by anesthesiologists and nurses.

2.2 Interventional Imaging Platform

The platform developed at NHLBI for interventional rtMRI utilizes clinical MR 1.5T scanners (Sonata with 8 receiver channels, Espree with 18 channels, and Avanto with 32 channels, Siemens Medical Solutions), with additional software for sockets communication over Gigabit Ethernet with a Linux workstation (8-CPU, 64-bit, AMD Opteron, HPC Systems, San Jose, CA) running custom software for rapid image reconstruction, display and 3D rendering [18;22]. The workstation is connected directly to the image reconstruction computer of the MR scanner for quick access to the raw echo data. The reconstruction and display software takes advantage of parallel processing by farming out tasks to different computing threads, which can run concurrently on different CPUs. Threads are created for individual processing of data from each receiver channel, combination of the data, graphical display, communications, and other tasks that can be executed in parallel. Open source packages and standards are used wherever possible: Fast Fourier transforms are performed using the FFTW library (fftw.org), graphics and user interface are implemented using OpenGL and GLUT (opengl.org).

At the beginning of a scan, imaging parameters are sent from the scanner to the workstation for initialization of the reconstruction program. At the end of each image acquisition, a packet of data is sent containing dynamic imaging parameters and the raw MR data. Commands are sent to the scanner in response to user input via the same network interface.

2.3 Data Acquisition and Image Reconstruction

MR data is acquired in the frequency domain (k-space) and reconstructed into an image by Fourier transformation. Real-time MR imaging requires an efficient pulse sequence, i.e. one that covers k-space in a short amount of time. This is often accomplished by acquiring many data points in each repetition, such as in echo-planar or spiral, or by using sequences with inherently short repetition times (TR), such as gradient-recalled echo or steady-state free precession (SSFP, a.k.a. True FISP, b-FFE, FIESTA) [23]. The NHLBI implementation uses SSFP for rapid, high SNR, consecutive imaging of multiple slices. Imaging parameters are adjusted to meet the requirements of the interventional procedure: although high frame rates are available, spatial resolution and image quality are often given priority over imaging speed, thus reported frame rates are well below the maximum attainable. The imaging frame rate is increased using variable rate view sharing or TSENSE [22;24]. TSENSE is one of several parallel imaging techniques such as SMASH [25], SENSE [26], and GRAPPA [27] which accelerate imaging by undersampling k-space and using the local sensitivity map of each coil element to either to fill in the gaps in k-space or remove undersampling artifacts in image space. Modern scanners feature 32 channels or more, which provide enough independent information for parallel imaging methods to achieve an acceleration factor of 2-4 with good image quality. Other acceleration methods do not require multiple coils and use the fact that the samples in a typical time series of image data are correlated in time (UNFOLD [28]) or both k-space and time (k-t BLAST [29]).

Since SSFP is a steady-state imaging sequence, care must be taken when disrupting the steady state for multiple slice imaging or image preparation such as fat suppression. In the NHLBI implementation for these cases, the magnetization is stored longitudinally (along the z-axis) after each image acquisition using a 'closing' sequence (-α/2; gradient spoil) [30], followed by the preparation and a series of RF pulses with gradually increasing flip angle on the new slice. Fat-

selective saturation is achieved by either a typical fat selective RF pulse or one of the quicker off-resonance saturation schemes as described elsewhere [31].

2.4 Real-time Imaging Features

Graphical user interfaces for rtMRI guidance of interventional procedures have been under active development. The first systems allowed basic real-time imaging with a single adjustable imaging plane [32;33]. Subsequent systems added many of the features described above [17-19;34]. Automatic image parameter adjustment in response to motion of a device being tracked has also been investigated [12;35].

A useful navigation technique using adaptively oriented projection navigation (PRONAV) was designed to facilitate steering of an active device towards target tissue. A device-only projection image and at least one standard thin-slice image are displayed together in a 3D rendering, all updated using real-time imaging. As the user interactively rotates the 3D rendering, the scanner automatically changes the projection direction, analogous to changing x-ray gantry position during fluoroscopy. This provides a real-time 3D view of the catheter position and trajectory with respect to the thin-slice image plane. For anatomical context, the thin-slice image is positioned to contain target tissue, and the combination of projection and thin-slice views can be used to navigate the device towards the target.

The NHLBI rtMRI implementation contains the projection imaging features and many other interactive features which can be controlled by simple keyboard or mouse operation without suspending imaging. Below is an abbreviated list of interactive features available [18;22;36]:

- Change slice position/orientation using the standard scanner slice prescription interface.
- Enable/disable acquisition of selected slices. This is used to trade-off frame rate for number of slices.
- Display each slice in separate windows as well as a 3D rendering where they are shown at their respective locations in space (see Figures 1 and 2). This provides simultaneous views of all slices and devices in one window, from any angle.
- Highlight device channels in different colors, blended with grayscale images from surface coils (see Figures 1 and 2). The device signal magnitude can be squared to sharpen the device profile.
- Mark reference points. Reference points are displayed as separate graphics objects like small colored spheres in the 3D rendering to mark anatomical features for device positioning and targeting (see Figure 2).
- Enable/disable squaring of device channel intensity. Squaring sharpens the device profile for more accurate localization.
- Enable/disable device-only projection view on selected slices to show entire device if it exits from the thinner imaging slice.
- Enable/disable adaptive projection navigation (PRONAV) mode for 3D projection views of the device.
- Use non-selective saturation to darken background and isolate T1-shortening contrast agent.
- Change acceleration factor.
- Enable subtraction imaging for enhancing contrast injections.
- Enable saving of raw data to files. The same program can be used at a later time to review the images with the same or different options for reconstruction or display. Several display and rendering parameters (such as 3D rendering orientation, highlight colors, window positions) are also saved. Post-procedure review therefore can mimic how the images were displayed during the actual procedure.
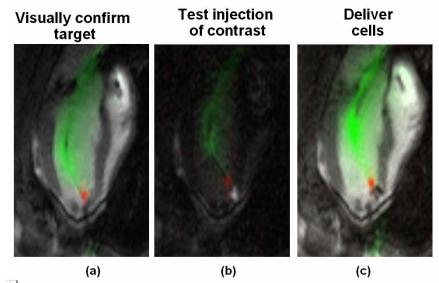
2.5 Communications and Image Display

Figure 1 shows the console room and magnet room (in the LCD display), showing the typical configuration during a surgical procedure in an animal model. Several displays are used in both the control room and the magnet room to view the real-time images, the scanner interface and physiology [37]. Team members wear custom-designed communication headsets (Magnacoustics, Atlantic Beach, NY) with noise-canceling optical microphones (Phone-Or, Or-Yehuda, Israel) to communicate during scanning for imaging parameter changes, timing during injections, or saving data. Slice position and orientation changes were performed interactively in the graphical prescription interface on the scanner console. The complexity of changing scanner parameters makes it necessary for an operator other than the physician to drive the scanner during the procedure, so good voice communication between the physician and operator is essential.

Figure 1. Pictures of the console room and inside the magnet room (seen on the LCD screen in front of the operator) during a swine experiment. The real time display is directly in front of the surgeon. The operator responds to voice commands through the voice activated microphone to change the scan plane views.

3. PRECLINICAL PROCEDURES

The system has been used by our group in a number of pre-clinical studies in swine, including endovascular repair of abdominal aortic aneurysms [36], stenting of aortic coarctation [38], recanalization of chronic total occlusions [39], atrial-septal puncture and balloon septostomy [40] and catheterization in humans [41]. An ideal application for MRI guidance in the heart is delivery and immediate visualization of intramyocardial injections of stem cells mixed with a contrast agent [6-8;42].

Visually confirm target **Test injection of contrast** **Deliver cells**
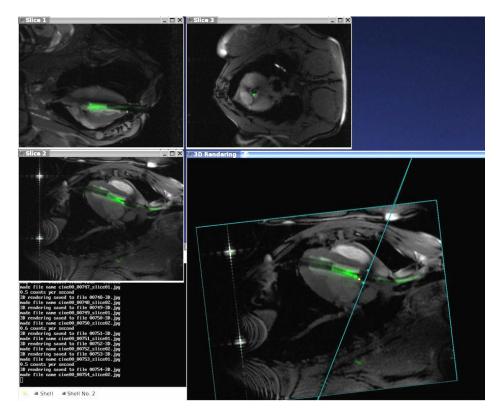
(a) (b) (c)

Figure 2 The targeting and visualization of intramyocardial injections. Each image is a single frame from a continuous real time MR movie. (a) The injection catheter in position with the distal tip against the myocardium. (b) A test injection with interactive saturation applied shows the contrast entering the myocardium. (c) The injection of labeled cells; the dark signal shows the presence of the cells.

Figure 2 shows an example of this type of application. The modified injection catheter is visualized with two active coils: the first gives signal along the shaft of the catheter, the second is a small localizer coil at the tip of the catheter. In

Figure 2(a) the position of the injection catheter is well visualized in this single frame from a realtime movie of the beating heart. In Figure 2(b), a test injection of Gd-DTPA contrast agent (diluted 100:1) is easily observed; in this case a saturation pulse was interactively toggled on during the injection. In Figure 2(c) the injection of 1cc of labeled mesenchymal stem cells is observed as a dark region due to the T2* contrast from the intracellular label [8].

Minimally invasive approaches to cardiac surgical therapies are under active investigation to reduce trauma and recovery time [43-45]. Therapies traditionally requiring open-chest access are now being carried out through small incisions. Without direct access to the target, approaches under development deploy robotic tools under the surgeon's control to administer therapy with fiber optics providing visual guidance. However, these approaches still require emptying the heart of blood to allow unobstructed visualization, and the heart is arrested to operate on a stationary target.
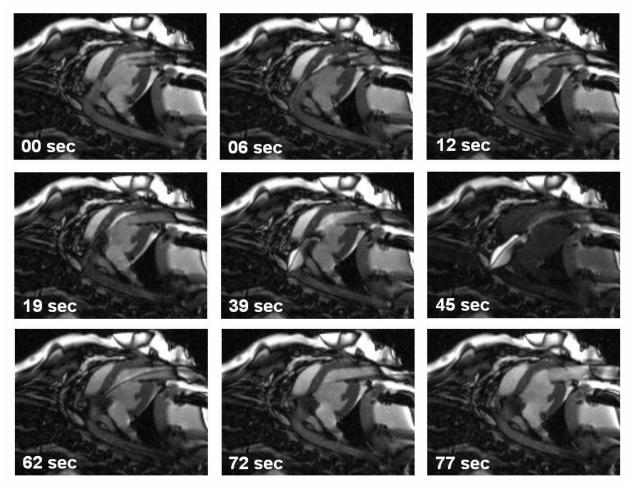

Figure 3. Three slices obtained in an interleaved fashion showing the position of the valve delivery device in the left ventricle. The top left view shows the trochar entering the apex of the LV, just below that view we can see the guidewire (green signal) passing beyond the aortic annulus, and in the view on the top we can see the aortic annulus in a short axis orientation with the valve positioned in its center. The 3D viewer shows the relationship of the short axis slice, and the anatomical markers on the long axis view. This 3D view can be interactively rotated to give the surgeon the desired views.

We have recently developed an imaging environment to guide the placement of a prosthetic aortic valve using a direct apical approach.[13] Figure 3 shows the views the surgeon uses to guide the delivery of the device to the aortic root. All of the images are a superposition of surface coil images with images obtained from a central active guidewire. The guidewire image is reconstructed in green to show the location of the wire. The prosthetic valve is rotated into position using the signal from the guidewire which is attached in a fixed location. The axial image provided feedback when rotating the valve to align the commissures of the valve between coronary ostia (cyan dots) before deployment.

The still images in Figure 4 are single frames extracted from the continuous real-time movie that is playing on the screen in front of the surgeon shown in Figure 1. Initially, a nitinol guidewire is advanced through the trocar across the native aortic valve, then the prosthetic stent-valve on the delivery device is advance through the apical trocar while

observing its location on the real-time MRI. The prosthetic valve is then advanced on the balloon, along the guidewire and positioned across the native valve in proper position with respect to the coronary artery ostia. The balloon is inflated using 1% diluted gadopentate dimeglumine (Gd-DTPA, Magnavist, Berlex Inc.) to implant the prosthetic valve under observation with real-time MRI. The balloon is then deflated and removed through the trocar. At this point the ventricular function resumes and it is visualized immediately on the real-time MRI.

Figure 4 Selected frames from the real-time MRI displayed within the scan room, showing the deployment of the prosthetic valve. (a) A guidewire is advanced through the trocar across the native aortic valve. (b) The prosthetic valve is advanced to the end of the trocar. (c) the prosthetic valve is advanced into position in the left ventricular outflow track. (d) the prosthetic valve is inserted across the native valve and aligned with the coronary ostia and the aortic annulus (e) a balloon filled with dilute Gd-DTPA MR contrast agent is used to expand the prosthetic valve (f) interactive saturation is used to enchance visualization of the extent of balloon inflation (g) the balloon is taken down and pulled back through the trocar (h) the guidwire is removed (i) the delivery device is removed from the trochar. The total time of this sequence of pictures is 77 seconds. (from McVeigh et. al. Magn. Reson. Med. 56(5):958 (2006))

4. DISCUSSION

An interactive real-time MR imaging environment initially developed for use in intravascular procedures [37] has been adapted to guide minimally invasive cardiovascular surgical procedures such as aortic valve placement. Many features were implemented that exploit the advantages of MRI: enhancing visualization of separate antennae or coils mounted on invasive devices, providing multiple oblique slices which are easily adjusted, rendering all slices and landmarks in 3D, accelerated imaging and projection imaging modes to see the entire trajectory of a device receiving signal along its shaft.

Real-time imaging of multiple oblique slices offers many potential advantages. Different views of complicated anatomy may be simultaneously displayed and individual slices can be interactively turned on or off during a scan as needed. This 3D rendering of multiple planes has been extremely useful for targeting devices. Another potential use is the continuous monitoring of cardiac function in one view during an intervention requiring a different view.

High performance hardware was used to minimize image reconstruction latency, which we estimate at approximately ¼ second. As reported, typical frame rates ranged from 3 to 8 per second, depending on choice of parameters. Much higher frame rates, in excess of 30 per second, were sustainable by the system when using small k-space matrix (such as 64 x 128), view sharing, and 8 receiver channels. This small matrix does not result in adequate image quality, but was useful to gauge the limits of the reconstruction and display pipeline. As of this writing, better raw data throughput and a faster reconstruction computer are required to handle real-time processing of 32-channel data with high acceleration rates and larger matrix.

The distinct advantage of MRI for guiding cardiac surgery is the fact that the surgeon can see "through" the blood, and all of the morphological landmarks for positioning the device are visible. The short magnet makes it possible to have high performance real-time MRI available while manipulating the prosthetic valve under image guidance. In addition to aortic valve replacements other target applications for real-time MR guided cardiac surgery are mitral, pulmonary and tricuspid valve replacements or repairs[46-49].

Future work will concentrate on the development of novel devices for both surgical and percutaneous access. Also, better fitting surface coils with optimally placed small coil elements will take advantage of the high number of receivers available on the newer MR imagers.

ACKNOWLEDGEMENTS

REFERENCES

1. Schulz T, Puccini S, Schneider JP, Kahn T. Interventional and intraoperative MR: review and update of techniques and clinical experience. *Eur Radiol*. 2004;..
2. Blanco RT, Ojala R, Kariniemi J, Perala J, Niinimaki J, Tervonen O. Interventional and intraoperative MRI at low field scanner--a review. *Eur J Radiol*. 2005;56:130-142.
3. Lardo AC, McVeigh ER, Jumrussirikul P, Berger RD, Calkins H, Lima J, Halperin HR. Visualization and Temporal/Spatial Characterization of Cardiac Radiofrequency Ablation Lesions Using Magnetic Resonance Imaging. *Circulation*. 2000;102:698-705.
4. Dickfeld T, Kato R, Zviman M, Lai S, Meininger G, Lardo AC, Roguin A, Blumke D, Berger R, Calkins H, Halperin H. Characterization of radiofrequency ablation lesions with gadolinium-enhanced cardiovascular magnetic resonance imaging. *J AM Coll Cardiol*. 2006;47:370-378.
5. Dickfeld T, Kato R, Zviman M, Nazarian S, Dong J, Ashikaga H, Lardo AC, Berger RD, Calkins H, Halperin H. Characterization of acute and subacute radiofrequency ablation lesions with nonenhanced magnetic resonance imaging. *Heart Rhythm*. 2007;4:208-214.
6. Lederman RJ, Guttman MA, Peters DC, Thompson RB, Sorger JM, Dick AJ, Raman VK, McVeigh ER. Catheter-based endomyocardial injection with real-time magnetic resonance imaging. *Circulation*. 2002;105:1282-1284.
7. Kraitchman DL, Sampath S, Castillo E, Derbyshire JA, Boston RC, Bluemke DA, Gerber BL, Prince JL, Osman NF. Quantitative ischemia detection during cardiac magnetic resonance stress testing by use of FastHARP. *Circulation*. 2003;107:2025-2030.

8. Dick AJ, Guttman MA, Raman VK, Peters DC, Pessanha BS, Hill JM, Smith S, Scott G, McVeigh ER, Lederman RJ. Magnetic resonance fluoroscopy allows targeted delivery of mesenchymal stem cells to infarct borders in Swine. *Circulation*. 2003;108:2899-2904.
9. Elgort DR, Hillenbrand CM, Zhang S, Wong EY, Rafie S, Lewin JS, Duerk JL. Image-guided and -monitored renal artery stenting using only MRI. *J Magn Reson Imaging*. 2006;23:619-627.
10. Henk CB, Higgins CB, Saeed M. Endovascular interventional MRI. *J Magn Reson Imaging*. 2005;22:451-460.
11. Lederman RJ. Cardiovascular interventional magnetic resonance imaging. *Circulation*. 2005;112:3009-3017.
12. Zuehlsdorff S, Umathum R, Volz S, Hallscheidt P, Fink C, Semmler W, Bock M. MR coil design for simultaneous tip tracking and curvature delineation of a catheter. *Magn Reson Med*. 2004;52:214-218.
13. McVeigh ER, Guttman MA, Lederman RJ, Li M, Kocaturk O, Hunt T, Kozlov S, Horvath KA. Real-time interactive MRI-guided cardiac surgery: Aortic valve replacement using a direct apical approach. *Magn Reson Med*. 2006;56:958-964.
14. Atalar E, Kraitchman DL, Carkhuff B, Lesho J, Ocali O, Solaiyappan M, Guttman MA, Charles HK. Catheter-tracking FOV MR fluoroscopy. *Magn Reson Med*. 1998;40:865-872.
15. Hillenbrand CM, Elgort DR, Wong EY, Reykowski A, Wacker FK, Lewin JS, Duerk JL. Active device tracking and high-resolution intravascular MRI using a novel catheter-based, opposed-solenoid phased array coil. *Magn Reson Med*. 2004;51:668-675.
16. Serfaty JM, Yang X, Aksit P, Quick HH, Solaiyappan M, Atalar E. Toward MRI-guided coronary catheterization: visualization of guiding catheters, guidewires, and anatomy in real time. *J Magn Reson Imaging*. 2000;12:590-594.
17. Aksit P, Derbyshire JA, Serfaty JM, Atalar E. Multiple field of view MR fluoroscopy. *Magn Reson Med*. 2002;47:53-60.
18. Guttman MA, Lederman RJ, Sorger JM, McVeigh ER. Real-time volume rendered MRI for interventional guidance. *J Cardiovasc Magn Reson*. 2002;4:431-442.
19. Quick HH, Kuehl H, Kaiser G, Aker S, Bosk S, Debatin JF, Ladd ME. Interventional MR angiography with a floating table. *Radiology*. 2003;229:598-602.
20. Kuehne T, Yilmaz S, Steendijk P, Moore P, Groenink M, Saaed M, Weber O, Higgins CB, Ewert P, Fleck E, Nagel E, Schulze-Neick I, Lange P. Magnetic resonance imaging analysis of right ventricular pressure-volume loops: in vivo validation and clinical application in patients with pulmonary hypertension. *Circulation*. 2004;110:2010-2016.
21. Cribier A, Eltchaninoff H, Tron C, Bauer F, Agatiello C, Nercolini D, Tapiero S, Litzler PY, Bessou JP, Babaliaros V. Treatment of calcific aortic stenosis with the percutaneous heart valve: mid-term follow-up from the initial feasibility studies: the French experience. *J AM Coll Cardiol*. 2006;47:1214-1223.
22. Guttman M, Dick A, Raman V, Arai A, Lederman R, McVeight E. Delayed Hyperenhancement Imaging without ECG-Gating or Breath Holding using Fast Interactive MRI [Abstract]. 2003.
23. Oppelt A. FISP - a new fast MRI sequence. *Electromedica*. 1986;54:15-18.
24. Kellman P, McVeigh ER. Ghost artifact cancellation using phased array processing. *Magn Reson Med*. 2001;46:335-343.
25. Sodickson DK, Manning WJ. Simultaneous acquisition of spatial harmonics (SMASH): fast imaging with radiofrequency coil arrays. *Magn Reson Med*. 1997;38:591-603.
26. Pruessmann KP, Weiger M, Scheidegger MB, Boesiger P. SENSE: sensitivity encoding for fast MRI. *Magn Reson Med*. 1999;42:952-962.
27. Griswold MA, Jakob PM, Heidemann RM, Nittka M, Jellus V, Wang J, Kiefer B, Haase A. Generalized autocalibrating partially parallel acquisitions (GRAPPA). *Magn Reson Med*. 2002;47:1202-1210.
28. Madore B, Glover GH, Pelc NJ. Unaliasing by fourier-encoding the overlaps using the temporal dimension (UNFOLD), applied to cardiac imaging and fMRI. *Magn Reson Med*. 1999;42:813-828.
29. Tsao J, Boesiger P, Pruessmann KP. k-t BLAST and k-t SENSE: dynamic MRI with high frame rate exploiting spatiotemporal correlations. *Magn Reson Med*. 2003;50:1031-1042.
30. Scheffler K, Heid O, Hennig J. Magnetization preparation during the steady state: fat-saturated 3D TrueFISP. *Magn Reson Med*. 2001;45:1075-1080.
31. Derbyshire JA, Herzka DA, McVeigh ER. S5FP: spectrally selective suppression with steady state free precession. *Magn Reson Med*. 2005;54:918-928.
32. Holsinger, A. E., Wright, R. C., Siederer, S. J., Farzaneh, F., Grimm, R. C., and Maier, J. K. Real-time interactive magnetic resonance imaging. Magn.Reson.Med. 14, 547-553. 1990.

33. Kerr A, Pauly J, Hu B, Li K, Hardy C, Meyer C, Macovski A, Nishimura D. Real-time interactive MRI on a conventional scanner. *International Society for Magnetic Resonance in Medicine, Book of Abstracts*. 1997;1:319.
34. Nayak KS, Pauly JM, Yang PC, Hu BS, Meyer CH, Nishimura DG. Real-time interactive coronary MRA. *Magn Reson Med*. 2001;46:430-435.
35. Elgort DR, Wong EY, Hillenbrand CM, Wacker FK, Lewin JS, Duerk JL. Real-time catheter tracking and adaptive imaging. *J Magn Reson Imaging*. 2003;18:621-626.
36. Raman VK, Karmarkar PV, Guttman MA, Dick AJ, Peters DC, Ozturk C, Pessanha BS, Thompson RB, Raval AN, DeSilva R, Aviles RJ, Atalar E, McVeigh ER, Lederman RJ. Real-time magnetic resonance-guided endovascular repair of experimental abdominal aortic aneurysm in swine. *J AM Coll Cardiol*. 2005;45:2069-2077.
37. Guttman M, Lederman RJ, McVeigh ER. The cardiovascular interventional MRI suite: design considerations. Lardo A, Fayad ZA, Fuster V, Chronos N, eds. 2003. Martin Dunitz.
38. Raval AN, Telep JD, Guttman MA, Ozturk C, Jones M, Thompson RB, Wright VJ, Schenke WH, DeSilva R, Aviles RJ, Raman VK, Slack MC, Lederman RJ. Real-time magnetic resonance imaging-guided stenting of aortic coarctation with commercially available catheter devices in Swine. *Circulation*. 2005;112:699-706.
39. Raval AN, Karmarkar PV, Guttman MA, Ozturk C, Sampath S, DeSilva R, Aviles RJ, Xu M, Wright VJ, Schenke WH, Kocaturk O, Dick AJ, Raman VK, Atalar E, McVeigh ER, Lederman RJ. Real-time magnetic resonance imaging-guided endovascular recanalization of chronic total arterial occlusion in a swine model. *Circulation*. 2006;113:1101-1107.
40. Raval AN, Karmarkar PV, Guttman MA, Ozturk C, DeSilva R, Aviles RJ, Wright VJ, Schenke WH, Atalar E, McVeigh ER, Lederman RJ. Real-time MRI guided atrial septal puncture and balloon septostomy in swine. *Catheter Cardiovasc Interv*. 2006;67:637-643.
41. Dick AJ, Lederman RJ. MRI-guided myocardial cell therapy. *Int J Cardiovasc Intervent*. 2005;7:165-170.
42. Hill JM, Dick AJ, Raman VK, Thompson RB, Yu ZX, Hinds KA, Pessanha BS, Guttman MA, Varney TR, Martin BJ, Dunbar CE, McVeigh ER, Lederman RJ. Serial cardiac magnetic resonance imaging of injected mesenchymal stem cells. *Circulation*. 2003;108:1009-1014.
43. Doty DB, Flores JH, Doty JR. Cardiac valve operations using a partial sternotomy (lower half) technique. *J Card Surg*. 2000;15:35-42.
44. Vassiliades TA, Jr., Block PC, Cohn LH, Adams DH, Borer JS, Feldman T, Holmes DR, Laskey WK, Lytle BW, Mack MJ, Williams DO. The clinical development of percutaneous heart valve technology: a position statement of the Society of Thoracic Surgeons (STS), the American Association for Thoracic Surgery (AATS), and the Society for Cardiovascular Angiography and Interventions (SCAI). *Ann Thorac Surg*. 2005;79:1812-1818.
45. Lutter G, Ardehali R, Cremer J, Bonhoeffer P. Percutaneous valve replacement: current state and future prospects. *Ann Thorac Surg*. 2004;78:2199-2206.
46. Cosgrove DM, III, Sabik JF, Navia JL. Minimally invasive valve operations. *Ann Thorac Surg*. 1998;65:1535-1538.
47. Mihaljevic T, Cohn LH, Unic D, Aranki SF, Couper GS, Byrne JG. One thousand minimally invasive valve operations: early and late results. *Ann Surg*. 2004;240:529-534.
48. Boudjemline Y, Agnoletti G, Bonnet D, Behr L, Borenstein N, Sidi D, Bonhoeffer P. Steps toward the percutaneous replacement of atrioventricular valves an experimental study. *J AM Coll Cardiol*. 2005;46:360-365.
49. Boudjemline Y, Bonhoeffer P. Images in cardiovascular medicine. Percutaneous aortic valve replacement in animals. *Circulation*. 2004;109:e161.